International Journal of Material Forming (2022) 15: 5
https://doi.org/10.1007/s12289-022-01648-w

ORIGINAL RESEARCH

Inverse heat transfer optimization of stamping with over-molding process involving high performance thermoplastic composites: experimental validation

Enrique Reyes[1,2] · Xavier Tardif[1] · Jean-Luc Bailleul[2] · Nadine Allanic[3] · Vincent Sobotka[2]

Received: 2 September 2021 / Accepted: 3 January 2022 / Published online: 28 January 2022

Abstract
Heat transfer plays a major role when designing manufacturing processes involving high-performance thermoplastic composites. Indeed, thermal parameters have a direct impact on part's quality and process productivity. Balance between these aspects remains a subject of study since more complex materials and hence more intricate processes emerge. Over the past decades, different optimization approaches have been proposed to overcome this challenge. Most of these investigations focused on a single stage of the process and the transformation of mono-materials. This research proposes a thermal design methodology that could be applied in all stages of the manufacturing process but also to a multi-material parts. The aim is to reduce defects inside manufactured pieces through the right configuration of thermal-related parameters, as temperature or heat flux distribution around the manufactured part at each stage. The designed methodology uses an inverse optimization algorithm based on a conformal cooling approach as proposed by Agazzi et al in Appl Thermal Eng 52(1):170–178, (2013) and Hopmann et al (2019). A 1D case is proposed to validate the methodology by comparing numerical results with experimental ones. A further extension to a 2D axisymmetric case is presented. Results for both 1D and 2D cases show an improvement of thermal profiles within the part. Temperature gradients could be reduced without decreasing bonding between elements for time dependent design variables. The thermal profile around the part could be used later to select the most adapted technology or cooling system.

Keywords Heat transfer · Inverse method · High performance thermoplastic composite · Optimization · Healing

Introduction

For a number of years, combining stamping with over molding techniques, in an almost simultaneous way, has become one of the best solutions to manufacture high-quality parts at a minimum production time. This task is achieved by merging the especial features of each technique in one single process. In the case of over-molding, a good quality surface could be obtained while reducing time by avoiding secondary operations such as drilling or cutting.

As show in Fig. 1, the stamping with over molding process can be summarized in 5 main stages. During the first stage, a composite sheet is preheated around the melting temperature. This operation can be realized in a convection oven or by infrared panels. In the second stage, the preheated sheet is transferred into the mold cavity. Then the preform is stamped and over-molded in the third and fourth stages respectively. In this last stage the assembly is cooled down and ejected. After part ejection, mold temperature could be raised again to reach the desired initial conditions of stamping in a fifth stage. Concerning the tooling, stages (3) to (5) as illustrated by Fig. 1, are repeated in a cyclic way. Metallic inserts could be integrated into the preform to add localized functions.

In these processes, significant attention has been oriented to the use of High-Performance ThermoPlastic Composites (HP-TPC). These materials with matrices such as PAEK

✉ Vincent Sobotka
vincent.sobotka@univ-nantes.fr

1 IRT Jules Verne, Chemin du Chaffault, 44340 Bouguenais, France

2 Nantes Université, CNRS, Laboratoire de thermique et énergie de Nantes, LTEN, UMR 6607, F-44000 Nantes, France

3 Nantes Université, CNRS, ONIRIS, GEPEA, UMR 6144, F-44000 Nantes, France

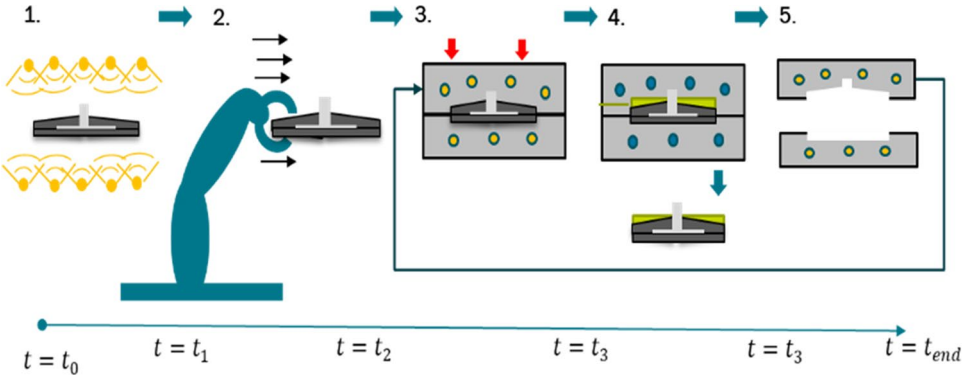

Fig. 1 Stamping with over-molding manufacturing process example. (A) Pre-heating (B) Transfer (3) Stamping (4) Over-molding (5) Mold temperature rise

are still subject of research [1]. They are very advantageous in applications where high multifunctional properties and thermal stability are required. However, HP-TPC have high melting point [2]. This implies that elevate temperature differences exist from the beginning to the end of the manufacturing process. This characteristic induces high cooling rates which can decrease polymer crystallization and can generate internal voids [3], reducing materials properties [4, 5]. Similarly, high temperature gradients within the part could appear whether during heating, consolidation or cooling stages. They may cause defects such as undesired residual stresses, shrinkage, fiber waviness, transverse cracks, delamination, or warpage [6] reducing quality of the manufactured parts [7].

Another aspect for which especial attention must be paid refers to the bonding [8] between constitutive elements. Good bonding is usually required between stamped composite sheet and injected polymers [9]. Bonding between polymers depends on two phenomena: the intimate contact and the degree of healing, which also depend on the thermal history [10]. Furthermore, appropriate definition of processing temperatures at each stage of the process is important as well. Temperature levels higher than required increase cycle time [11], not to mention possible material degradation.

The impact of temperature on quality and productivity is well-known. Nevertheless, to avoid the aforementioned problems, a fundamental issue remains to obtain a suitable process design according to the heating /cooling requirements for each stage of the process. To overcome this challenge, optimization algorithms, whether stochastic, deterministic, or a combination of both have been used to improve either process conditions or cooling system design [7, 12, 13]. In this last area, it has been demonstrated that the conformal cooling approach is a powerful method when compared with conventional techniques. This method seeks to design cooling channels adapted to the part shape [7]. Their fabrication is possible thanks to 3D printing manufacturing methods. Conformal channels reduce temperature gradients because they allow a better heat flux distribution around the part, helping to attain a quality part and process productivity. Inspired by the conformal cooling approach, Agazzi et al [12] propose a morphological cooling approach. This approach is based on the creation of a contour dilated zone called "Dilation" around the part, as illustrated by Fig. 2. The generation of this zone helps to design cooling channels without previous knowledge about their number, shape, location and fluid temperature [12]. At the same time, it reduces computational time since heat transfer evolution in not computed in the entire mold. The thickness of the dilated zone is created at a constant distance from the part's surface thanks to a structuring element. The external line of the dilated zone is called, cooling line, Γ_3 on the Fig. 2. In the same way, an internal boundary, also called "erosion", is created. The closed eroded segment is used to establish a target condition inside the part. Erodes lines are placed at a constant distance from the part surface as well. Following, an inverse optimization method that uses a first-order deterministic algorithm is implemented. The design variable is located on the cooling line. The variable is supposed constant in time. The cost function to be minimized is composed by two terms. These terms refer to the target temperature required at the eroded segment for productivity; and the

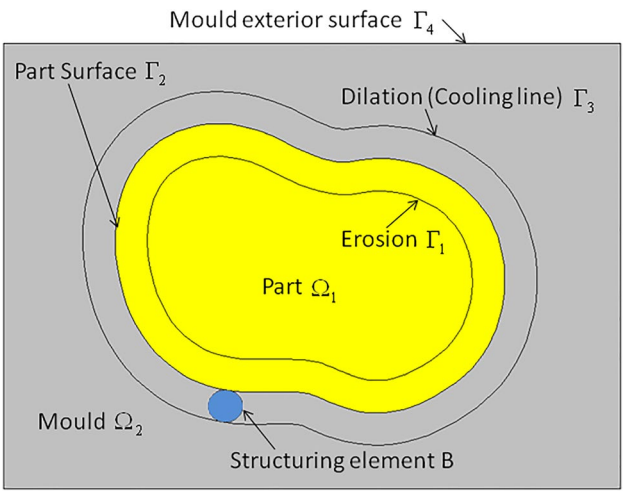

Fig. 2 Morphological cooling approach by Agazzi et al. [12]

uniform temperature distribution required at the mold-part interphase for quality. The obtained optimized profile in the dilated zone is later used for the conformal channel's design.

The methodology proposed by Agazzi [12] was extended by Hopmann et al [14]. In their work, they took into account mold opening and closing times, proven the versatility of the methodology. But instead of uniform temperature distribution, a density homogeneity of the polymer minimizing the difference between local densities was proposed as quality criteria.

In this work, we seek to extend the aforementioned methodology to find optimized boundary conditions, as a function of time and space. The methodology is applied to the main stages of a combined manufacturing process. Thus, contrary to the previous investigations, the generation of a dilated zone is not required in all steps of the optimization procedure. In addition, the integration of an optimization criterion based on bonding between elements is explored. The first part of this paper introduces the methodology. After describing its formulation, it is validated on an experimental process for further application on a constrained 1D case. Then the methodology is applied to a 2D axisymmetric study case of thermo-stamping with over molding of a metal insert of HP-TPC as represented in Fig. 1.

Inverse heat transfer optimization methodology

In the present methodology, an inverse optimization algorithm is implemented. Geometry construction adapted to hybrid manufacturing process is explained. Optimized heat flux or temperature distributions in time and space are obtained by minimizing a cost function that depends of thermal related parameters. The optimization procedure is performed in sequence, starting from the first stage to the final stage of the process. In this way, optimized results of one stage are used as initial conditions for the optimization of the following stage.

Geometry creation

As done by Agazzi et al. [12] geometry generation including eroded and dilated zones constitutes the first step of the methodology. As explained earlier, in their investigation a dilated zone surrounding the part was created (see Fig. 2). The external surface of this zone was used to locate the design variable. Dilated distance must be long enough to avoid thermal stresses in the mold while ensuring sufficient mechanical resistance during the molding process. Influence of the dilated distance have been studied previously [12]. Nevertheless, in hybrid manufacturing process, dilated zone change depending on the analyzed stage. For this reason, when no mold is present, design variables are set directly in the external surface of the work piece, as illustrated in Fig. 3a by surfaces $\Gamma_3 \bigcup \Gamma_4$. The thickness of the dilated zone is at a constant distance of the final part geometry (Fig. 3c). This means that in previous stages the dilated zone is not necessary a homothetic representation of the part (Fig. 3b). In this case, special care must be taken to avoid excessive geometry differences between the part geometry and the dilated zone's shape. Furthermore, final part is composed by more than one material. Each material represents one domain on the final geometry (Fig. 3c). These domains are taken into account according to the corresponding stage as detailed in Fig. 3. For the preheating and transfer stages only the (Ω_1) domain is analyzed. In the stamping stage the problem is solved for the preform (Ω_1) and dilated (Ω_2) domains. Following, eroded segments must be created at each part domain of the work piece. Eroded segments could be partitioned to enable cost function evaluation according to the optimized stage. Position of the eroded segment from the part surface depends on the objective function.

Design variable definition

The boundary condition used in the dilated surface can be an imposed temperature, heat flux or mixed condition. In this work it was chosen to impose a Newton condition at the

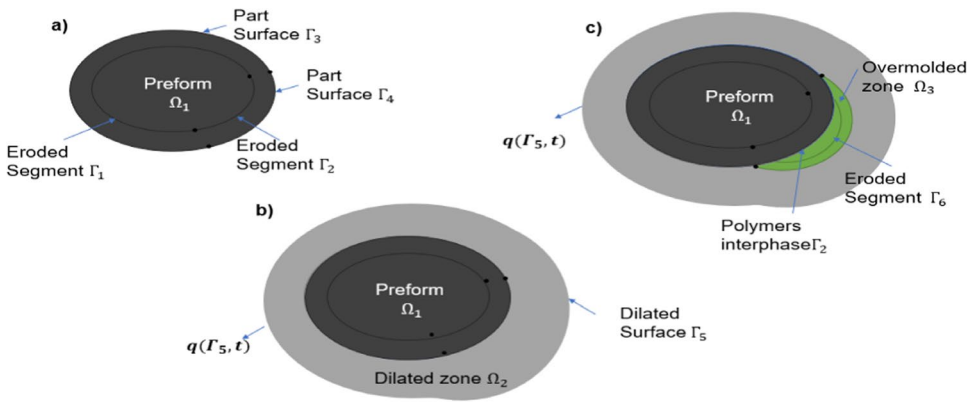

Fig. 3 Geometry creation adapted to hybrid processes: **a** preheating-transfer. **b** Stamping. **c** Over-molding and cooling

external boundary of the study geometry: $-\lambda \frac{\partial T}{\partial n}\Big|_{\Gamma} = h\left(T_{\Gamma} - T_{\infty}\right)$where T_{∞} is the searched design variable and h a fixed heat transfer coefficient as done by [12, 14].. This variable is searched as a function of time and/or space depending of the studied case. This condition does not in any way foresee the technology that will be chosen to achieve the thermal regulation system after the optimization. It makes it possible to estimate the heat flux at the dilated surface by considering an equivalent heat transfer coefficient h as well as the temperature T_{∞}.The heat flux obtained from this boundary condition could help later on the selection of an adapted processing technology. In addition, the design variable could be searched to reach a target condition on a subsequent stage of the process. As an example, optimized heat fluxes could be determined on the preheating stage (step 1 in Fig. 1) to reach a target condition on the transfer stage (step 2 in Fig. 1).

Cost function evaluation

In this study, three terms are considered in the cost function: target temperature, maximum degree of healing and temperature homogeneity, as indicated by the terms in equations set (1). Second and third terms correspond to quality criteria while the first term is associated with a productivity criterion.

$$\begin{aligned} J\left(T_{\infty}\right) = \alpha \int_{\Gamma_{eroded}} \int_{tf-\tau}^{tf} \left\| T_{target}\left(t_f\right) - \mathbf{T}\left(T_{\infty}\right) \right\|^2 dt d\Gamma_{eroded} \\ + \beta \int_{\Gamma_p} \int_{tf-\tau}^{tf} \left\| 1 - D_h\left(T_{\infty}\right) \right\|^2 dt d\Gamma_p \\ + \gamma \int_{\Gamma} \int_{tf-\tau}^{tf} \left\| \overline{\boldsymbol{T}}\left(T_{\infty}\right) - \boldsymbol{T}\left(T_{\infty}\right) \right\|^2 dt d\Gamma \end{aligned} \quad (1)$$

In the above equation α, β and γ are weighting factors. These factors help to set convergence rates for each term of the cost function, as expressed by [15]. *tf*, is the final time of the stage where the cost function is evaluated. T_{target}, is the target temperature. Γ_{eroded}, is the corresponding eroded segment according to the optimized stage. In the example presented in Fig. 3a. $\Gamma_{eroded} = \Gamma_1 \bigcup \Gamma_2$. Γ_p, is the interphase between polymers. $D_h(T_{\infty})$, is the degree of healing. $\mathbf{T}(T_{\infty})$, is the temperature field in the part and $\overline{\mathbf{T}}\left(T_{\infty}\right)$ its average value. This temperature depends on the design variable, T_{∞}, which depends on time and space; Γ_5 is the part external surface.

Algorithm implementation

Inverse optimization problem is solved based on a first-order deterministic algorithm known as the conjugate gradient (see Fig. 4). This method is applied on the constructed geometry. To start, two direct problems are treated: a thermal direct problem and a healing direct problem. The latter is considered as bonding indicator between the composite sheet and over-molded polymers. The obtained solutions are used to evaluate the cost function. Gradient expression is afterwards obtained through a Lagrangian formulation called adjoint state and solved backwards in time. Subsequently, deepest descent is computed at each iteration step based on the sensitivity analysis. The optimization loop is performed for each design variable of the process.

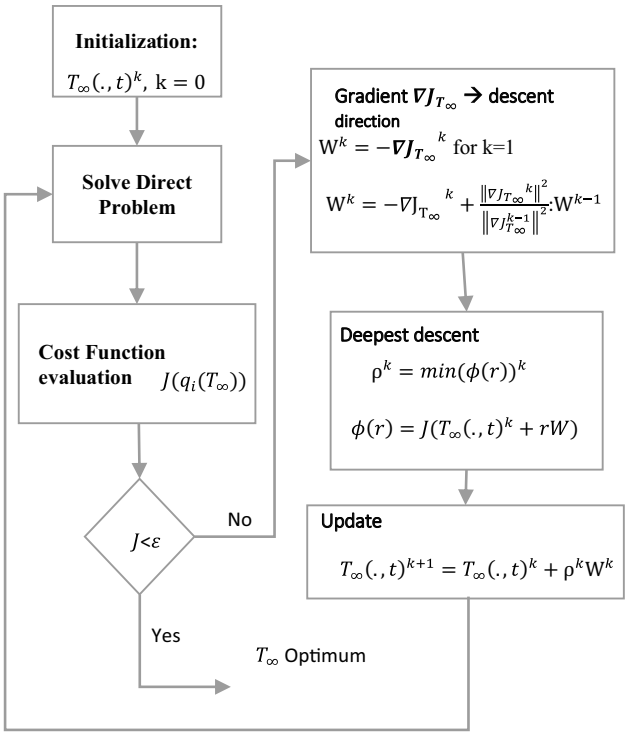

Fig. 4 Conjugate gradient algorithm applied to each optimization block. Adapted from [14]

Direct thermal problem

Temperature field evolution is obtained solving the classical heat transfer diffusion equation with no source generation:

$$\rho_i(T) Cp_i(T) \frac{\partial \mathbf{T}_i(.,t)}{\partial t} = \nabla.\left(\lambda_i(T) \nabla \mathbf{T}_i(.,t)\right) \quad \forall i = 1 \ldots n \quad (2)$$

Where i, corresponds to each domain either the composite or the dilated part; $\rho_i(T)$, $Cp_i(T)$, $\lambda_i(T)$ are the temperature dependent properties and; $\mathbf{T}i$ (., t) the corresponding temperature field in each domain. Number of domains n depend

on the constitutive elements of the final part plus the dilated domain.

Direct healing model

Healing has been defined as the process where the interphase of contact materials is eliminated by interdiffusion of polymers chains creating a monolithic structure. This phenomenon was modelled throughout the reptation theory [16]. Based on this theory, Yang et al [9], explain that a total bonding could be reached at the welding time for high molecular weight materials. In this way, it replaces the reptation time by a welding time on the Healing Degree expression, as detailed in Eq. 3.

$$D_h(t) = \left(\frac{t}{t_\omega(T)}\right)^{1/4} \tag{3}$$

This model has been used as well by Avenet et al [16] in the adhesion bonding of high-performance thermoplastic composite. It can be expressed in the differential form [8, 16] as:

$$dD_h^4(t) = \frac{1}{t_\omega(T)}dt \tag{4}$$

Where $t_\omega(T)$ is the temperature dependent welding time classically modelled using Arrhenius law:

$$t_\omega(T) = k^{\left(\frac{E_a}{RT}\right)} \tag{5}$$

k, E_a, R and T are respectively a material constant, the activation energy, the universal gas constant and the temperature. Healing degree is numerically calculated based on the thermal history obtained from the direct thermal model.

Gradient expression

The gradient expression is obtained throughout the adjoint state [17]. This technique is useful when an explicit relationship between the design variable and the cost function variables is not easy to obtain. The adjoint state equations are found from the following Lagrangian expression:

$$\mathcal{L}(\mathbf{T}_\infty, \mathbf{\Psi}_i) = J(\boldsymbol{T}_\infty) - \left(\sum_{i=1}^{n}\int_{t_{0,i}}^{t_{f,i}}\left\langle \rho_i Cp_i\frac{\partial \mathbf{T}_i}{\partial t} - \nabla.\lambda \mathrm{i}\nabla\mathbf{T}_i, \mathbf{\Psi}_i\right\rangle_{\Omega \mathrm{i}}\right) \tag{6}$$

Where Ψ is the adjoint variable; t_0, and t_f, are the initial and final times in which each domain "i" is activated. The set of the adjoint equations and the gradient expression are then obtained considering a fixed Ψ so we can have$\delta\mathcal{L}(\mathbf{T}_\infty, \mathbf{\Psi}_i) = \delta J(\boldsymbol{T}_\infty)$. When the adjoint variable is fixed the Lagrangian satisfies:

$$\delta\mathcal{L}(\mathbf{T}_\infty, \mathbf{\Psi}_i) = \sum_{i=1}^{n}\frac{\partial\mathcal{L}}{\partial\mathbf{T}_i}\delta\mathbf{T}_i + \frac{\partial\mathcal{L}}{\partial\mathbf{T}_\infty}\delta\mathbf{T}_\infty \tag{7}$$

Then, $\mathbf{\Psi}$ is chosen to verify

$$\frac{\partial\mathcal{L}}{\partial\mathbf{T}_i}\delta\mathbf{T}_i = 0 \ \ for \ \ i = 1\ldots n \tag{8}$$

An explicit relation of the gradient is then found as a function of the adjoint variable, as expressed in Eq. 9. The obtained gradient expression depends on the boundary condition on the surface where the design variable is searched. In our case, for the defined Newton boundary condition the discretized gradient expression is as follow:

$$\boldsymbol{\nabla J}_{\boldsymbol{T}_\infty mn} = \sum_{m=1}^{p}\sum_{n=1}^{q} - h\psi\left(\Gamma_n, t_m\right)d\Gamma_n dt_m \tag{9}$$

Where p and q, are the number of maximum spatial and temporal components of the gradient. h is the heat transfer convective coefficient and ψ the adjoint variable.

Sensitivity analysis

The sensitivity problem is solved using Eq. 10. It plays three roles on the implementation of the methodology. First, it allows to know if the cost function variables are sensitive enough to the design variable placed at the external surface of the analyzed part (see Fig. 3). If not, design variable or its location should be changed, otherwise the methodology could not be conducted. This information is crucial since it determines whether or not the methodology could be applied. Secondly, it is useful to obtain an adapted deepest descent in the algorithm implementation as suggested by [12, 18]. Obtained expression for the deepest descent depends of the cost function definition as detailed in Eq. 11 for one term of the cost function. Finally, the number of time components (p) of the gradient expression is chosen based on the sensitivity analysis as well. For a given number of components, sensitivity of the resulted time range must be high enough to perform the optimization.

$$\rho_i(T)Cp_i(T)\frac{\partial\delta\mathbf{T}_i(.,t)}{\partial t} = \Delta\left(\lambda_i(T)\delta\mathbf{T}_i(.,t)\right)\forall i = 1\ldots n \tag{10}$$

$$\rho^k = \frac{\nabla J^k_{\boldsymbol{T}_\infty} * w^k}{\alpha\int_{tf-\tau}^{tf}\int_{\Gamma Eroded}\left(\delta T^2\right)^k d\Gamma_{eroded}dt} \tag{11}$$

Experimental process description

A laboratory stamping process of a HP-TPC is used to validate the methodology. The process attempts to weld two thermoplastic composite samples. It is divided into

five stages as illustrated by Fig. 5. In the first stage, two samples of organosheets are preheated in a convection oven. The samples are then transferred and positioned into a mold cavity. In the subsequent stage, the mold is closed to consolidate the assembly. Parts are cooled down in the last stage.

Experimental apparatus

A fan-assisted convection oven has been used for the samples preheating. The oven is a commercial Universal Oven XU032. Its maximum heating temperature is 300 °C. For the bonding and cooling stages, a workbench developed at the laboratory has been employed (Fig. 6). The workbench was originally designed for welding under isothermal conditions. Fixed and mobile ends as presented in Fig. 6, are made of cooper. Heating panels are placed at 10 mm from the cavity's surface while thermocouples are placed at 1 mm from the same surface. Cooling channels are conventional. Further details on the mold bench can be found in [19].

Materials

Two samples of carbon fiber reinforced high-performance thermoplastic were used. They were obtained from an organosheet made of aeronautical grade Arkema PEKK 7002 thermoplastic with 12 plies of symmetric unidirectional fiber layup of [0°/90°]. Samples with the same properties were used in a previous study on the adhesion of high-performance thermoplastic composites made by Avenet et al [16].

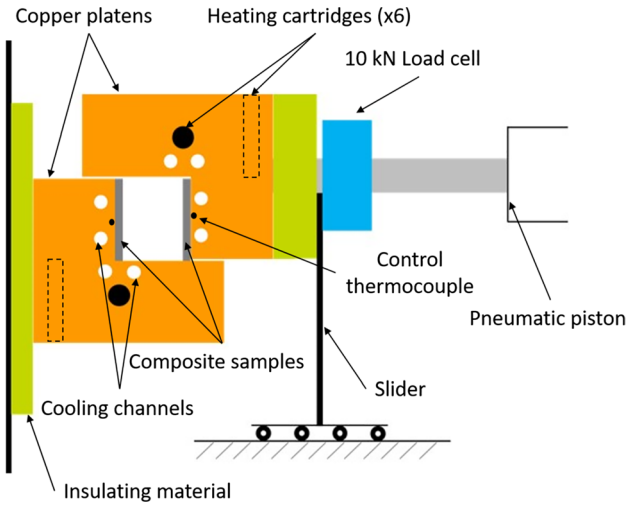

Fig. 6 Experimental Bench [19]

Instrumentation

Samples were instrumented with 80μm K-type thermocouples placed at mid-width of each sample at half thickness and on top and bottom surfaces, giving a total of 4 thermocouples named (T1, T2, T3, and T4) as indicated in Fig. 7. Thermocouples T2 and T3 are set to verify temperature values at the interphase between the two samples.

Process parameters

During the preheating stage the oven is set to its maximum temperature of 300 °C. In the bonding stage, the mold temperature is set at 340 °C. Finally, in the cooling stage, cooling is achieved with water at room temperature until

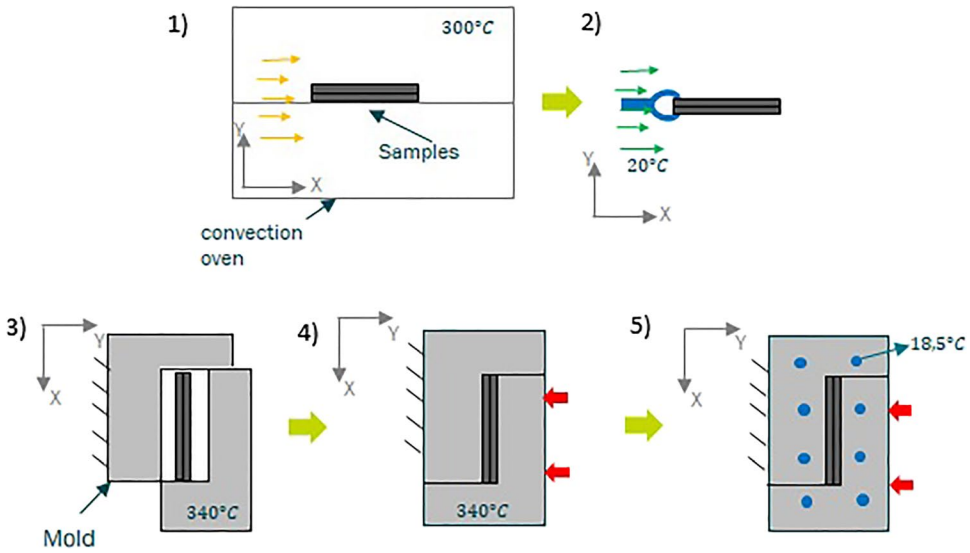

Fig. 5 Experimental process description. (1) Preheating (2) Transfer (3) positioning (4) Bonding (5) Cooling

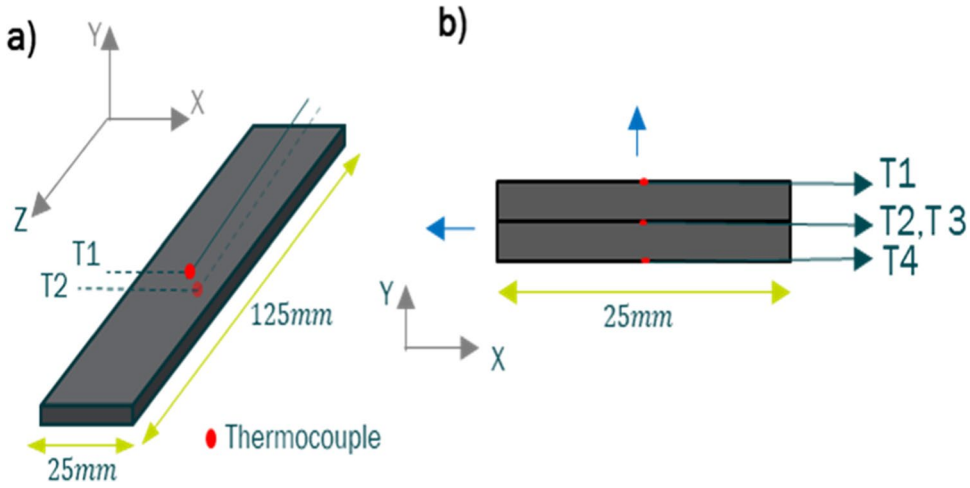

Fig. 7 Thermocouple's placement. **a** Isometric view of one sample **b** Transversal view of superposed samples

Table 1 Process parameters

Stage	Processing time (s)	Process Temperature (°C)	Process Variable
Preheating	586	300	T_{∞}
Transfer	28	22	$T_{\infty 2}$
Bonding	10	340	$T_{\infty 3}$
Cooling	>10	18,5	$T_{\infty 4}$

the stationary temperature evolution is reached. Processing parameters are specified in Table 1.

Methodology validation

Geometry creation

Considering the transversal and longitudinal symmetry of the mold cavity and the samples (see Figs. 6 and 7), the process is analyzed as a one-dimensional problem, as illustrated in Fig. 8. Sample's properties are considered thermo-dependent. Following the previous description of the methodology, one single geometry is created for solving all the stages of the process. Eroded is represented by a point placed at $y=0$ i.e. in the middle of the composite assembly that represents the interface between the two samples where Dh is evaluated. The domains are activated according to the studied stage. For the preheating and transfer stages only the first domain (Ω_1) is activated. For the other stages, the distance of the dilated zone corresponds to the separation between the mold cavity and the heating panels in the mold bench.

Direct model

Direct thermal model is solved using Eq. 2. Third kind boundary conditions are set according to heat transfer hypotheses for each stage. For the preheating and transfer stages, convective and radiative heat transfer exchanges, as detailed in Eq. 12 were imposed over the first domain's external boundary (6th node in Fig. 8).

$$-\mathrm{n}.\lambda_1(T)\nabla T_1 = h_i\left(T_1 - T_{\infty i}\right) + \varepsilon\sigma\left(T_1^4 - T_{\infty i}^4\right)\forall i = 1,2 \tag{12}$$

In the above equation, i correspond to the stage number in Fig. 5. Consequently, $T_{\infty 1}$ correspond to the oven temperature, fixed at 300 °C, during the preheating stage. On the transfer stage the surrounding temperature $T_{\infty 2}$, is the room temperature fixed at 22 °C. Following, during the bonding stage, the initial mold temperature is considered homogenous at 340 °C. In this stage, the third kind boundary condition detailed in Eq. 13 is imposed at the outer boundary of the dilated zone (7th node in Fig. 8). Temperature $T_{\infty 3}$

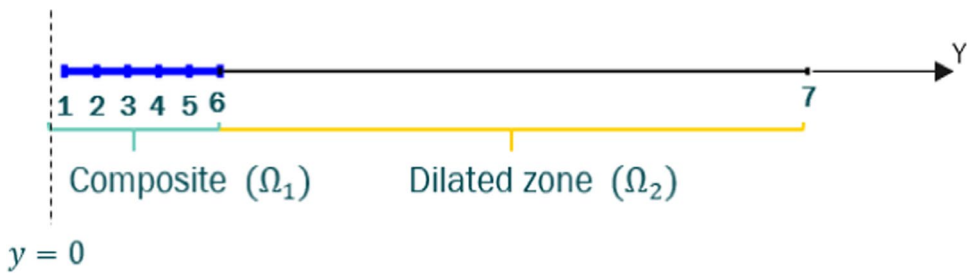

Fig. 8 1D geometrical configuration

at the surroundings is chosen to be 340 °C as well, which is the temperature evolution used to heat the experimental bench. Convective heat transfer coefficient h_3 was set to 10000 W/m^2K to guaranty an imposed temperature condition $T_{\infty 3}$ as done by [12].

$$-\mathrm{n}.\lambda_2(T)\nabla T_2 = h_3\left(T_2 - T_{\infty 3}\right) \tag{13}$$

In the same way, a Thermal Contact Resistance (TCR) is imposed between the mold cavity and the composite sample surface. Afterwards, an identification of experimental process parameters h_1 and h_2 as well as the TCR was carried out. Found values were set to fit the experimental temperature evolution over time, as listed in Table 2. Finally, during the cooling stage, ambient temperature is set at the outer boundary of the dilated zone (Ω_2) until the time required to reach room temperature.

In this study, the positioning stage is not taken into account. As a matter of fact, manual transfer of the composite samples causes a non-controlled positioning into the mold cavity. As a consequence, unpredictable contact zones creating conductive and convective heat transfer occurs during this stage. For this reason, temperature values obtained in the experimental test at the end of the positioning stage, are directly set as initial condition for the bonding stage. Despite of this, the validation procedure of the methodology is not affected.

Thereafter, healing degree is numerically calculated using Eq. 4. In this equation, temperature evolution corresponds to the collected temperature values from the experimental bonding stage. Numerical formulations of the direct and healing models was solved using the finite element method on COMSOL Multiphysics®. After solving the direct model, the maximum difference between the experimental and numerical temperature evolution was about 15 °C during the first quarter of the preheating stage. Difference at the final time of the preheating stage was less than 1 °C. For the bonding stage a maximum temperature difference of 5.1 °C was obtained (Fig. 9).

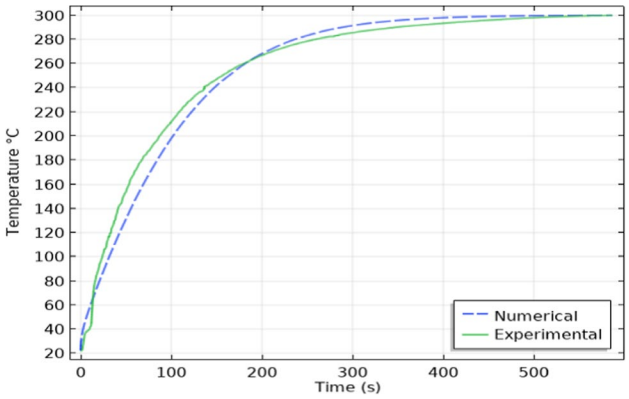

Fig. 9 Comparison o of experimental (solid line) and numerical (dashed line) results during the preheating stage

Design variable and cost function definition

For the validation procedure two design variables are defined: the oven temperature $T_{\infty 1}$, at the preheating stage; and the mold temperature $T_{\infty 3}$ in the bonding stage. Thus, two optimization loops must be executed. The first optimization considers the preheating and transfer stages as one problem. Second optimization loop is executed on the bonding stage. In this stage searched variable $T_{\infty 3}$ is supposed time dependent. Subsequently, the cost function is defined. For the first optimization, only the primary term of Eq. 1 is used. This cost function is evaluated during the transfer stage. For the second case, the cost function is a combination of target temperature and degree of healing. The degree of healing is required at the eroded point (node 1 in Fig. 8) while target temperature is required at mold-part interphase (node 6 in Fig. 8). The sensitivity analysis proves that healing degree at the bonding interphase is less sensitive to the design variable than the temperature profile at the external surface. For this reason, the value of β must be higher than α . In both optimization cases, the target temperature is the experimental temperature T1 (Fig. 7) gathered at the final time of the stage where the design variable is searched. The optimum degree of healing is calculated from the experimental thermal history. For this reason, the later replaces the unit in Eq. 1. Finally, the optimization loop aims to identify experimental oven temperature and mold temperatures set points.

Table 2 Process parameters

Stage	Parameter	Identified Value
Preheating	h_1	22 W/m^2K
Transfer	h_2	14 W/m^2K
Bonding	$RTC_{mold-composite}$	$1.3x10^{-3}m^2K/W$
Cooling	$RTC_{mold-composite}$	$6x10^{-4}\ m^2K/W$

Comparison between experimental and optimized results

In this section we evaluate the capability of the methodology to find the experimental oven and mold temperatures set points. The validation of the methodology is divided into two parts. First, the inverse optimization procedure is applied to the preheating and transfer stages. The second inverse optimization is computed on the bonding stage.

Preheating and transfer stages

As stated previously, the optimization was carried out using only the first term of the cost function (See Eq. 1).

Table 3 Preheating-Transfer temperature values

	$T(t_f)$ (°C) Transfer	T_∞ (°C) Preheating	$T_\infty^{k=0}$
Optimized	247.8	299	356.85
Experimental	247.8 (Target Condition)	300 (Searched variable)	

The target temperature $T_{target}(t_f)$ in this term corresponds to the collected experimental temperature on the top surface of the composite sample. This temperature was given by the thermocouple T1 at the end of the transfer stage, as detailed on Table 3. The design variable was initialized at $T_{\infty 1}(t)^{k=0}$=356.85 °C and considered constant in time. As can be seen from Table 3, the experimental and optimized temperatures at the end of the preheating stage are in very good agreement.

Bonding stage

For this optimization case the target degree of healing and the temperature at the final time for the cost function evaluation are specified in Table 4. The design variable $T_{\infty 3}$ is time dependent.

The optimization problem is run for a number of gradient time components p equals to 3 (See Eq. 9). The selection is based on the sensitivity problem. Chosen times, in seconds, were [629.5; 632; 634.5]. Linear interpolation of the searched variable is made between the selected points. The initial guess for the design variable was initialized for all points at $T_{\infty 3}^{k=0}$= 486.9 °C at the iteration k = 0. After the optimization procedure, it can be observed from Table 5 that the experimental set points values in Table 4 are found with an acceptable relative error, defined by the objective function. This implies that time discretization of the gradient expression can be used to found a time dependent design variable. Found values of the time dependent temperature are plotted in Fig. 10.

Application of the methodology to a constrained optimization problem

After methodology validation, time dependent design variable is searched in order to have a maximum healing degree with a minimum temperature gradient over the thickness. For this reason, second and third terms of the cost function presented in Eq. 1 are used. Nevertheless, for the last term, temperature

Table 4 Bonding target values

Method	$D_h(t_f)$	$T(t_f)$ (°C)
From Experimental	0.43 (Target Condition)	331.9 (Target Condition)

Table 5 Bonding stage-validation results

$D_h(t_f)$	$T(t_f)$ (°C)	$J(T_{\infty 3})$ (m.s)
0.43	337.0	$18x10^{-2}$

homogeneity is required over the thickness instead of the external surface Γ. Three time components of the design variable are searched. Number of points were set using the sensitivity analysis. Linear interpolation between the components of the design variable is made while constant extrapolation is made outside the selected times.

Constraints

The optimization problem is subjected to two constraints: upper and lower temperature limits and maximum cooling and heating rate. These constraints are described as follow:

$$20°\mathrm{C} < T_{\infty 3} < 500°C \tag{14}$$

$$-1.4°C/s < {dT_{\infty 3}}/{dt} < 1.4°C/s \tag{15}$$

These limits were set according to the workbench capabilities in terms of maximum temperature and maximum power rate.

Optimization results

As can be seen in Table 6, the use of the inverse technique leads to a reduced temperature difference ΔT over the thickness without compromising the degree of healing D_h at the final time t_f .The temperature difference ΔT is obtained between the 1st and 6th node in Fig. 8 which correspond to the interphase of the two composites samples and the mold-part interphase. The found parameters $T_\infty(t)$ in degree

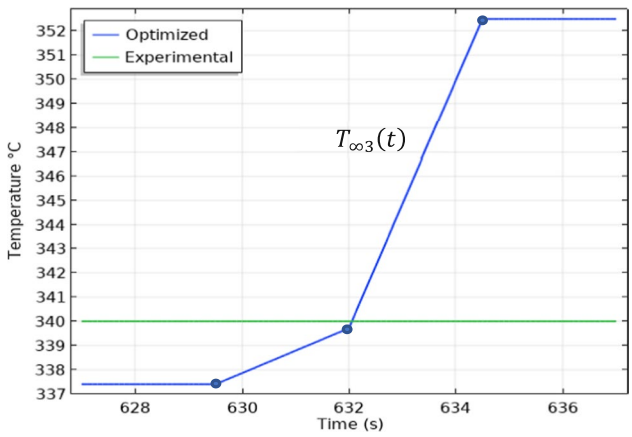

Fig. 10 Comparison between experimental and optimized design variable $T_{\infty 3}(t)$

Table 6 Bonding stage- optimization results

Method	$D_h(t_f)$	$\Delta T(t_f)$ (°C)	$J(T_\infty)$ (m.s)
Optimized	0.43	19.0	$6.4x10^{-2}$
Non-Optimized	0.43	20.6	–

Celsius were [343.5 340 336.5] at the corresponding times [629.5 632 634.5]. More flexible constraints or increased times could lead to a reduced temperature gradient over the thickness and a higher degree of healing.

Further extension of the methodology to a 2D axisymmetric case

Problem description

For the 2D application a stamping with over-molding process as illustrated in Fig. 1 is chosen as an application example. During the preheating (stage 1), the preform is heated over the melting point. For this reason, the surrounding temperature T_∞ is chosen to be 350 °C as indicated in Table 7. Then, it is transferred into the mold cavity (stage 2). Temperature at the surroundings during this stage is defined as $T_{\infty 2}$. During the stamping stage (stage 3), initial mold temperature is defined as T_{mold} while the temperature at the outer surface of the dilated zone is defined as $T_{\infty 3}$. During over-molding stage (stage 4), the boundary condition temperature is labelled $T_{\infty 4}$. In this stage, polymer is injected at the injection temperature T_{inj} . After cooling, mold temperature is raised again at a surrounding temperature $T_{\infty 5}$. Values of these process parameters are summarized in Table 7. Processing times were chosen according to a hybrid manufacturing process unit.

Geometry creation

The geometry is studied as a 2D axisymmetric problem as shown in Fig. 11. Four domains are created. They correspond to the metal insert (Ω_1), the composite organosheet (Ω_2), the dilated zone (Ω_3) and the over-molded

Table 7 Process parameters

Stage	Processing time (s)	Value (°C)	Process parameter
Preheating	90	350	T_∞
Transfer	6	20	$T_{\infty 2}$
Stamping	6	340	T_{mold}
		340	$T_{\infty 3}$
Over-molding and cooling	25	360	T_{inj}
		140	$T_{\infty 4}$
Temperature rise	65	340	$T_{\infty 5}$

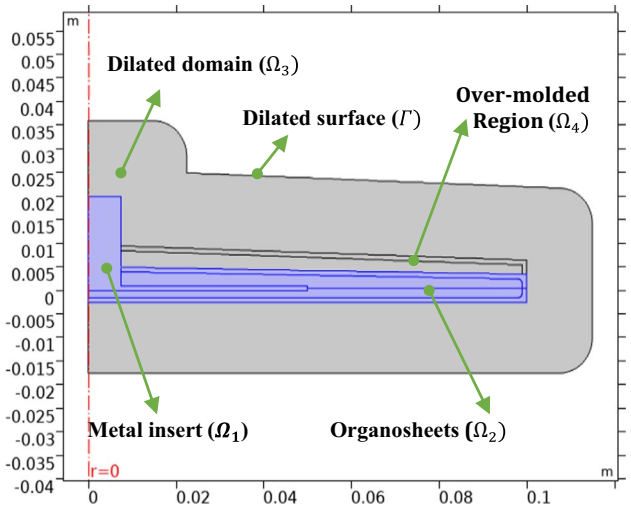

Fig. 11 2D Study case. Multi-material approach

polymer (Ω_4). Following the proposed methodology, two partitioned eroded segments are created. Only the domains present in a particular stage are analyzed. The dilated surface (Γ) is placed at 15 mm from the part surface. The eroded segments are created at 1 mm from the part surface. During stamping and over molding this distance is chosen so as to guarantee a solid thickness from the part surface before ejection [21]. Composites sheets and over-molded region are 2 mm thick.

Numerical model

The model is solved in COMSOL Multiphysics® using Eqs. 2, 6 and 8 for the direct problem, the adjoint state and the sensitivity problem respectively. Material properties were considered constant as listed in Table 8.

Boundary conditions are established according to the hypotheses made for each stage as follow:

- **Preheating stage**: radiative and convective exchanges between the composite and surroundings were considered in a global heat transfer coefficient.

Table 8 Material Properties

Part	Material	Conductivity (λ) $W/(m.K)$	Density (ρ)kg/m^3	Heat Cap. (Cp)$J/(kg.K)$
Metal insert	Aluminum	238	2700	900
Organo-sheet	PEEK-CF	Long 3 Trans:0.7	1464	1148
Mold	Steel	44,5	7850	475
Polymer	PEEK	0,25	1320	1340

- **Transfer stage:** a global heat transfer coefficient is obtained for a fixed transfer time. This coefficient depends on the speed and trajectory of the part. During this stage process parameters such as, time t, heat transfer coefficient h and surrounding temperature $T_{\infty 2}$ are considered known.
- **Stamping stage:** the mold temperature at the initial is considered homogenous at 340 °C for the first cycle. Its value is chosen according to the temperature required within the part to guarantee a bonding condition [20]. Thermal Contact Resistances (TCR) are imposed between all the elements. Composite deformations are not taking into account. The analysis only focuses on the heat transfer.
- **Over-molding:** An injection temperature for the melted polymer is fixed to 360 °C. No phase change is assumed. Over-molding time comprises packing phase and cooling. The over molding required time is calculated based on the thermal diffusion time on the dilated zone.

Design variable

In this study case, 3 design variables are defined. T_{∞} at the preheating stage; $T_{\infty 5}$ on the temperature rise stage and $T_{\infty 4}$ for the over-molding stage . Therefore, 3 optimizations loops are performed. For the first and second optimizations the design variables are considered constant in time and depending on space. These optimizations regroup two stages of the process. Preheating and transfer for the first optimization and temperature rise and stamping for the second optimization. The last optimization supposes a time dependent design variable.

Objective function and constraints

In this study, the objective function is composed of the two terms: target temperature at the respective eroded segments and uniform temperature distribution at the mold-part interphase depending of the studied stage. The chosen objectives correspond to the first and third terms on Eq. 1. The target temperatures that are desired at the final time of each stage are listed in Table 9. Bonding condition is not taken into account while performing 2D optimization during the over-molding stage because a lack of sensitivity.

The optimization problem is subjected to upper and lower temperature limits as expressed in Eq. 16. These constraints are imposed at each optimization.

Table 9 Target values for the cost function

Stage	Transfer	Stamping	Over-molding
Target temperature (°C)	347	340	230

$$\min limit \leq \mathbf{T}_{\infty}(\Gamma, t) \leq \max limit \tag{16}$$

Lower level is set to 20 °C and upper level to 500 °C. These limit levels were imposed to all optimization loops.

Analysis of results

Optimization of the preheating and transfer stages

In this optimization, infinite temperature $T_{\infty 1}$ distribution during the preheating stage was determined in order to reach the desired target condition at the end of the transfer stage. Figure 12 illustrates optimized and non-optimized profiles on the eroded segment of the composite domain. The non-optimized condition is obtained considering a constant value, in time and space, of the surrounding temperature $T_{\infty 2}$ that allows to reach the desired target temperature. In this way, for the non-optimized case $T_{\infty 2}$ is fixed to 377 °C on Γ.

Maximum temperature difference over the A-B segment was 4.5 °C. This temperature is found at the contact zone between the polymer and the metal insert. Temperatures differences are about 1.5 °C from the top and bottom surfaces compared to a maximum value of 12 °C for the non-optimized case, proving a reduction of temperature differences and confirming the advantage of the methodology.

Optimization of the temperature rise-stamping stages

During the stamping stage, the cost function variable $T_{target}(t_f)$ searched at the eroded segment is not sensitive enough to the process variable $T_{\infty 3}$ placed in the outer boundary of the dilated zone. In fact, due to the small duration of stamping stage, temperature profile evolution within the part depends more on the mold initial conditions than the temperature at the dilated external surface. Initial mold

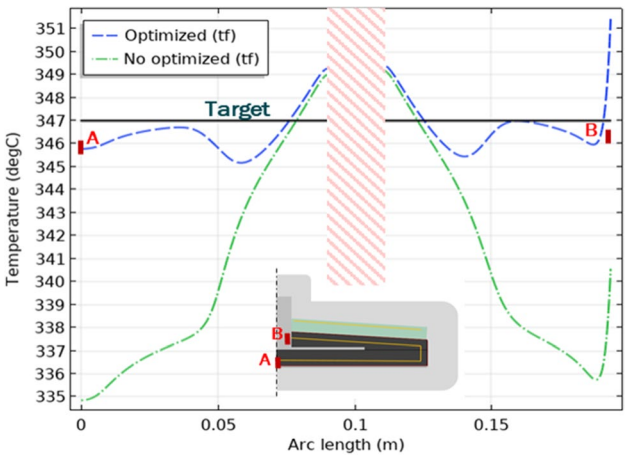

Fig. 12 Optimized and non-optimized profiles at the end time of the transfer stage

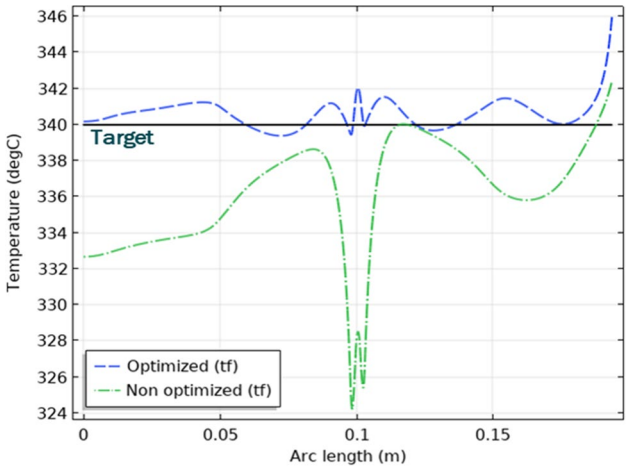

Fig. 13 Optimized and non-optimized profiles at the end of the stamping stage

temperature corresponds to the final temperature profile of temperature rising stage. For this reason, temperature rise stage and stamping stages are analyzed as one problem. This reconfiguration is possible thanks to the cycle evolution on the process. Figure 13 plots temperature profiles evolutions over the internal boundary A-B (See Fig. 12) at the end of the stamping stage. In here a maximum of 5 °C deviation with respect the target condition was found. The algorithm stabilizes at 8 iterations, as detailed in Fig. 14.

Optimization of the over-molding stage

During over-molding, an optimized infinite temperature $T_{\infty 4}$ distribution varying in time and space was found. As general rule, time components should be chosen to guarantee sensitivity. In this case, a minimum of time range of 5 s is established based on the sensitivity analysis. Fig. 15 shows the optimized infinite temperature distribution. Knowing this temperature, the heat flux can be then determined using Eq. 11. Concerning the target criteria (230 °C) an average temperature of 229.4 °C is obtained after optimization, in contrast with 223.2 °C before optimization. Maximum and minimum temperatures over the eroded segment were less than 5 °C from the target temperature, proving in this way that an improvement of the temperature profile is obtained when using the design variable as a time and space function.

Conclusion

A thermal design methodology aiming to find space and/or time dependent temperature/heat flux distributions is proposed. Its application is focused on hybrid manufacturing process involving multiple materials. A stamping with over-molding manufacturing process is chosen as an application example. The methodology enables the use of a single geometry to analyze all the stages of the process. Contrary to the previous investigations [12, 14, 15], design variables are found as a function of time and space. Dilated zone is not required in all the stages of the optimization procedure.

Fig. 14 Converge plot

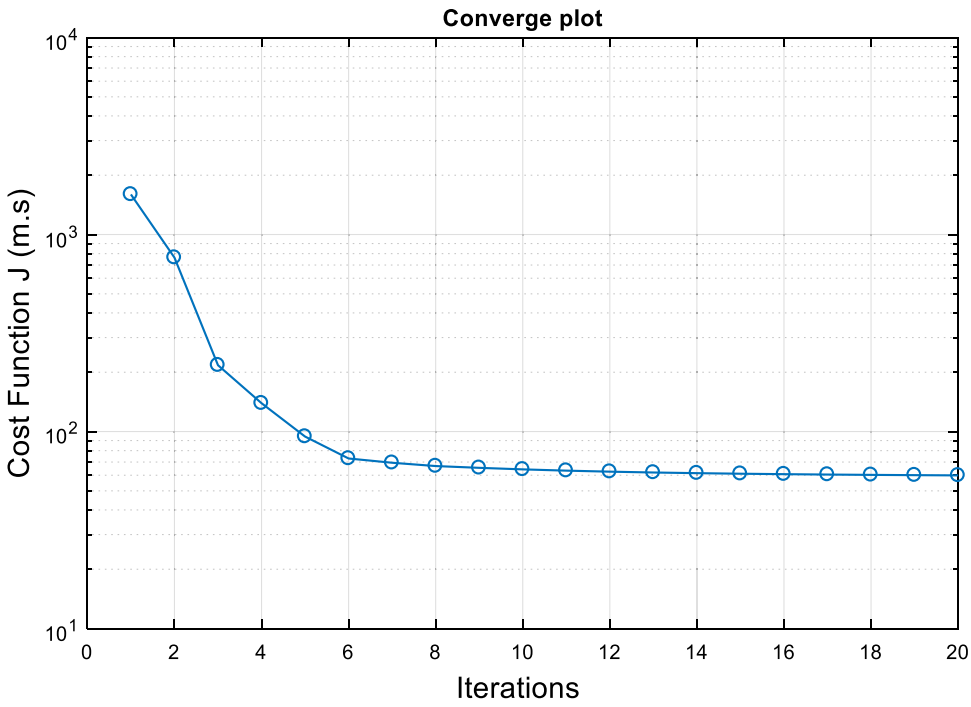

The methodology was validated throughout an experimental test and applied to a constraint optimization problem in one and two dimensions. In this application, an improvement of cost function was achieved when minimizing the target temperature, the temperature homogeneity and healing degree according to the study case. Ground rules for selection of the number of time partitions of the design variable were introduced. The optimized condition is intended to guide on the later construction of conformal channels and on the selection of an appropriate cooling/heating technology. Implementation on the methodology in a 3D case in ongoing.

Supplementary Information The online version contains supplementary material available at https://doi.org/10.1007/s12289-022-01648-w.

Acknowledgements The authors would like to thank Julien Avenet for the help on the set up of the TACOMA workbench.

Funding This work was funded by the PERFORM program managed by the IRT Jules Verne (French Institute for Research and Technologies for composite, Metallic and Hybrid Structures) as well as their associated partners of the PERFORM project: Airbus, Daher Europe Technologies, Faurecia, Loiretech Naval Group, SAFRAN and Stelia Aerospace.

Declarations

Conflict of interest The authors have no conflicts of interest to declare that are relevant to the content of this article.

References

1. Prosofsky de Araujo G, Donadon MV, Salerno G, Sales, R. de C. M. (2021) Temperature effects on the mechanical behaviour of PAEK thermoplastic composites subjected to high strain rates under compression loading. Compos Struct 261(November 2020):113299
2. High Performance Polymers/Overview. http://www.chinaarray.com/HPTP.html
3. Manson J-AE, Schneider TL, Seferis JC (1990) Press-forming of continuous-fiber-reinforced thermoplastic composites. Polym Compos 11(2):114–120
4. Bessard E, Almeida ODe (2011) Etude et modelisation de la cinetique de cristallisation du PEEK lors de refroidissements isothermes et anisothermes:
5. Zopp C, Nestler D, Buschner N, Mende C, Mauersberger S, Tröltzsch J et al (2017) Influence of the cooling behaviour on mechanical properties of carbon fibre-reinforced thermoplastic / metal laminates. Technologies for Lightweight Structures 1(2):32–43
6. Parlevliet PP, Bersee HEN, Beukers A (2006) Residual stresses in thermoplastic composites—a study of the literature—part I: formation of residual stresses. Compos A: Appl Sci Manuf 37(11):1847–1857
7. Park SJ, Kwon TH (1998) Optimal cooling system design for the injection molding process. Polym Eng Sci 38(9):1450–1462
8. Yang F, Pitchumani R (2002) During thermoplastic fusion bonding. Polym Eng Sci 42(2):424–438
9. Joppich T, Menrath A, Henning F (2017) Advanced molds and methods for the fundamental analysis of process induced Interface bonding properties of hybrid, thermoplastic composites. Procedia CIRP 66:137–142
10. Yang F, Pitchumani R (2003) Nonisothermal healing and Interlaminar bond strength evolution during thermoplastic matrix composites processing. Polym Compos 24(2):263–278
11. Mehnen J, Micheltisch T, Bartz-Beielstein T, Schmitt K (2004) Evolutionary optimization of mould temperature control strategies: encoding and solving the multiobjective problem with standard evolution strategy and kit for evolution algorithms. Proc Inst Mech Eng B J Eng Manuf 218(6):657–665
12. Agazzi A, Sobotka V, LeGoff R, Jarny Y (2013) Optimal cooling design in injection moulding process – a new approach based on morphological surfaces. Appl Therm Eng 52(1):170–178
13. Park HS, Nguyen TT (2015) Optimization of injection molding process for car fender in consideration of energy efficiency and product quality. J Comput Des Eng 1(4):256–265
14. Hopmann C Nikoleizig P (2019) Inverse thermal mold design for injection molds
15. Hopmann C, Gerads J, Hohlweck T (2021) Investigation of an inverse thermal injection mould design methodology in dependence of the part geometry. International Journal of Material Forming:309–321
16. Avenet J, Cender TA, Le Corre S, Bailleul JL, Levy A (2020) Adhesion of high temperature thermoplastic composites. Proc Manuf 47(2019):925–932
17. Jarny Y (2002) The adjoint method to compute the numerical solutions of inverse problems. In: Woodbury KA (ed) Inverse engineering handbook. CRC Press, Boca Raton, FL
18. Rehfahi AK (2000) Resolution numérique de problems inverse 2D non linéaires de conduction de la chaleur par la méthode des éléments finis et l'algorithme du gradient conjugué. Validation expérimentale. Ecole polytechnique de l'université de Nantes
19. Avenet J, Levy A, Bailleul JL, Le Corre S, Delmas J (2020) Adhesion of high performance thermoplastic composites: development of a bench and procedure for kinetics identification. Compos A: Appl Sci Manuf 138(July)
20. Jarrousse G (2004) Self adhesion of semi-crystalline polymers between their glass transition temperature and their melting temperature. PhD Thesis, vol. 1, no. 1,p. 254